Finite difference schemes comparison on the drying process of a banana

Maria Rosa Amorim Faria Lisboa[1], Gessica Starepravo Xambelan[1], Fernando Enrique Castillo Vicencio[1], Luciano Nappa Padilha Siqueira[1], Viviana Cocco Mariani[1]

[1]*Department of Mechanical Engineering, Pontifical Catholic University of Paraná*
R. Imaculada Conceição, 1155 - Prado Velho, 80215-901. Paraná/Curitiba, Brazil
lisboa.maria@pucpr.edu.br, xambelan.gessica@pucpr.edu.br, fernando.vicencio@pucpr.edu.br,
luciano.siqueira@pucpr.edu.br, viviana.mariani@pucpr.br

Abstract. Drying is an ancient method for preserving fruit and vegetable crops. It has been used effectively to extend the lifespan of agricultural products and decrease post-harvest losses. Drying, or dehydration, consists in lowering the vegetable's moisture content by evaporation. This procedure reduces microorganisms' reproduction and other reactions that would result in rapid deterioration of organic matter. Therefore, it conservates food for longer periods of time. During drying, complex phenomena occurs then mathematical modeling and simulation are adequate tools to study the product's behavior. In this instance, this work aims to compare three Finite Difference schemes (Crank-Nicolson, Dufort-Frankel and Euler explicit) on how suitable they are for describing the behavior of a banana during drying. The numerical results obtained were compared to experimental data.

Keywords: Thermal diffusivity, banana, numerical method, drying, food.

1 Introduction

Drying is a well-known, ancient method of preserving fruit and vegetable crops by decreasing spoilage, and can be used effectively to extend the shelf life of agricultural products (fruits and vegetables) and decrease their post-harvest losses [1]. Furthermore, from an economic point of view, high quality dehydrated products can be produced and stored at relatively low costs, which makes them suitable for today's competitive global market.

Since banana is a fruit produced in most countries with tropical climate, it is the target of numerous researches on the drying process. Drying can be described as a complex chemical phenomenon, and although it focuses on creating a stable product in most approaches, it consumes a lot of energy, accounting for about 15% of overall production costs [2]. Importantly, these techniques are associated with higher greenhouse gas emissions, representing a serious threat to the environment. This justifies the numerous researches that have been carried out with the objective of increasing the quality of the final product, reducing the drying time and reducing the dryer's energy supply costs from renewable sources [3].

To describe layer drying of agricultural products, we can divide into two main groups of models. The first group corresponds to empirical models and the second corresponds to diffusion models. Empirical models are important not only for describing thin-film water removal, but also for describing the penetration of heat during such removal when hot air is used. In this case, heating is guided by the diffusion equation, which involves the drying rate in the energy balance [4, 5], and this rate can be determined by an empirical model.

As already mentioned, drying is a complex phenomenon and, therefore, mathematical modeling and simulation are tools to deal with this complexity. Mathematical modeling in fruit drying consists of using mathematical equations to predict the operation procedure [6]. Several parameters must be defined for the mathematical modeling of drying. Castro *et al.* [7] describe these parameters in their article. These parameters must be generated during the design of the model before starting a mathematical modeling.

For the determination of thermophysical parameters, such as effective diffusivity and mass transfer coefficient, an adequate mathematical model must be adapted to the description of the drying kinetics of a product. Empirical models can be used to determine such parameters [8, 9]. In the case of the liquid diffusion model, an optimization algorithm, based on the inverse method can be used [5, 10, 11].

Mariani *et al.* [5] proposed an optimization algorithm for determining the apparent thermal diffusivity of bananas using a numerical solution of the diffusion equation. Silva *et al.* [11] proposed two algorithms, one deterministic and the other stochastic, to determine the diffusivity of effective drying mass of mushrooms, using an analytical solution of the diffusion equation for an infinite slab with boundary conditions of the first type.

For simple geometries such as plates, cylinders and spheres with constant thermophysical properties, simple analytical and numerical solutions can be found in researches such as Silva *et al.* [12], although when the real geometry is replaced by a simple geometry, an analysis of the moisture or temperature distributions cannot be fully accepted, as they do not provide information about the internal deformation or crack formation in the product. Thus, some moisture diffusion studies are carried out using a real product geometry, thus identifying regions critical to cracks. It is noteworthy that while an infinite cylinder allows to predict the distribution of moisture only in the central region, the real geometry allows the distribution of moisture at the ends of the product [13].

Numerical and analytical methods are used to approximate the solution of partial differential equations. The three main successful numerical methods are finite differences, finite volume and finite elements. Analytical models to solve decoupled mass transfer equations in 1D. de Lima *et al.* [14] used the finite volume method to describe the process, considering the shrinkage and an ellipsoidal configuration for the product. Silva *et al.* [15] also studied the drying of whole bananas using the finite volume method applied to an ellipsoidal geometry, but their model considered effective moisture diffusivity as a variable property.

For numerical analysis, explicit and implicit methods are used. Implicit models when dealing with non-linearity of material properties, need to perform sub iterations, thus increasing the total number for convergence, *e.g.* Janssen [16], which needed thousands of iterations to converge a solution for mass diffusion. On the other hand, an explicit scheme allows a direct calculation of the solution at the next time. An example of work based on explicit schemas is Tariku *et al.* [17] propose a model of calorie and moisture transfer taking into account protective effects such as protection against moisture, moisture sources and the effects of moisture on calorie transfer.

Defining the geometry and dimension of the system is essential. Although there are researches as seen before where the geometry used is the closest to the fruit, most researchers use a rectangular or cylindrical shape, it is noteworthy that when using a cylindrical geometry it is common to take an infinite cylinder.

In order to make comparisons and determine the accuracy of the models, we can find in the literature the following statistical indicators such as: coefficient of determination (R2), mean average error (MAE), the mean average percentual error (MAPE) and root mean square error (RMSE).

2 Numerical Discretization

One-dimensional heat and mass transfer in polar coordinates may be represented as a parbolic model based on Fourier and Fick equations for heat and mass diffucion, respectively [5].

$$\frac{\partial T}{\partial t} = \frac{1}{r}\frac{\partial}{\partial t}\left(r\alpha\frac{\partial T}{\partial r}\right) \tag{1}$$

$$\frac{\partial X}{\partial t} = \frac{1}{r}\frac{\partial}{\partial t}\left(rD_{ef}\frac{\partial X}{\partial r}\right) \tag{2}$$

Equations 1 and 2 can be discretized in space and time, as shown in Fig. 1

2.1 Crank-Nicholson implicit scheme

In turn, the Crank-Nicholson discretization [18]—based on the trapezoidal rule—is an implicit scheme—in time and space—widely applied in diffusion problems. This method is unconditionally stable.

2.1.1 Heat transfer in the banana

Applying both of derivatives of first and second order in Eq. 1:

$$\left(\frac{\partial T}{\partial t}\right)_{i,j+\frac{1}{2}} = \frac{\alpha}{r}\frac{\partial}{\partial r}\left(r\frac{\partial T}{\partial r}\right)_{i,j+\frac{1}{2}} \tag{3}$$

At this point, the Crank-Nicolson approach can be applied in the Eq. 3. In this case, it is the equivalent of the average of two time steps on the spatial derivative —RHS of the Eq. 3.

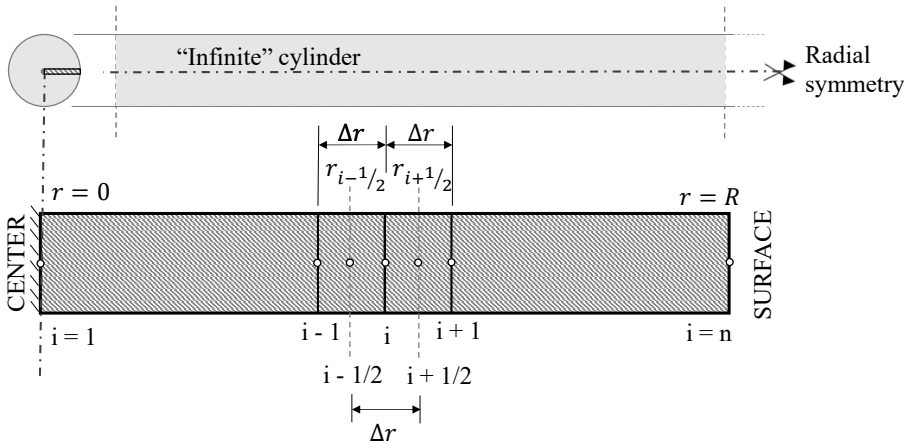

Figure 1. Radial discretization.

$$\frac{T_i^{j+1} - T_i^j}{\Delta t} = \frac{\alpha}{r}\frac{1}{2}\left[\frac{\partial}{\partial r}\left(r\frac{\partial T}{\partial r}\right)_{i,j+1} + \frac{\partial}{\partial r}\left(r\frac{\partial T}{\partial r}\right)_{i,j}\right] \tag{4}$$

Rearranging Eq. 4, we get an implicit expression that can be solved with some tridiagonal system os equations (TSOE) slver, as TDMA, Gauss-Siedel or Gaussian elimination.

$$\frac{T_i^{j+1} - T_i^j}{\Delta t} = \frac{\alpha}{2r\Delta r^2}\left[r_{i+\frac{1}{2}}\left(T_{i+1}^{j+1} + T_{i+1}^j - T_i^{j+1} - T_i^j\right) - r_{i-\frac{1}{2}}\left(T_i^{j+1} + T_i^j - T_{i-1}^j + T_{i-1}^{j+1}\right)\right] \tag{5}$$

In this work, these TSOE will be solved by using the TDMA solver.

Boundary condition at $r = 0$ $(i = 1)$ can be obtained from the Maclaurin expansion, resulting in this expression:

$$\frac{T_1^{j+1} - T_1^j}{\Delta t} = \frac{2\alpha}{\Delta r^2}\left(T_2^{j+1} + T_2^j - T_1^{j+1} - T_1^j\right) \tag{6}$$

For $r = R$ $(i = n)$, the boundary condition is obatined for energy balance at the external surface, consisting on inlet convection and outlet energy by heat convection and mass transport:

$$-k\left.\frac{\partial T}{\partial r}\right)_n = h\left(T_n - T_e\right) + \rho_s \Delta r \frac{\partial \overline{X}}{\partial t}\left[h_{fg} + c_v(T_n - T_e)\right] \tag{7}$$

Rearranging Eq. 7 to obtain the forward temperature at the time $j + 1$:

$$T_n^{j+1} = \frac{T_{n-1}^{j+1} + \frac{h\Delta r}{k}T_e - \frac{\rho_s \Delta r^2}{k}\left(\frac{\overline{X}^{j+1} - \overline{X}^j}{\Delta t}\right)\left[h_{fg} + c_v T_e\right]}{1 + \frac{h\Delta r}{k} + \frac{\rho_s \Delta r^2}{k}\left(\frac{\overline{X}^{j+1} - \overline{X}^j}{\Delta t}\right)c_v} \tag{8}$$

2.1.2 Mass transfer in the banana

Analogously to the heat transfer, the mass transfer at the internal elements—similar to Eq.‘5.

At the center of the banana, $r = 0$ $(i = 1)$, can be calculated similarly to Eq. 6:

$$\frac{X_1^{j+1} - X_1^j}{\Delta t} = \frac{2D_{ef}}{\Delta r^2}\left(X_2^{j+1} + X_2^j - X_1^{j+1} - X_1^j\right) \tag{9}$$

On the other hand, the mass balance is calculated by the diffusion equation:

$$-D_{ef}\frac{\partial X}{\partial r} = h_m(X_R - X_e) \tag{10}$$

In this way, the boundary condition at the external surface of Eq. 10 can be obtained by forward difference:

$$-D_{ef}\frac{X_n^{j+1} - X_n^j}{\Delta t} = h_m(X_n^{j+1} - X_e) \tag{11}$$

2.2 Explicit forward Euler scheme for heat and mass diffusion

The Euler explicit scheme can also be applied to solve the diffusion Eq. 1 and 2, but it must be taken into account the following stability requirement [19, 20] for heat transfer:

$$\frac{\alpha\Delta t}{\Delta r^2} \leq \frac{1}{2} \tag{12}$$

Thus, with the forward explicit method applied to Eq. 1 at the internal elements, the following point-to-point expression can be obtained:

$$\frac{T_i^{j+1} - T_i^j}{\Delta t} = \frac{2\alpha}{\Delta r^2}\left(T_{i+1}^j - 2T_i^j + T_{i-1}^j\right) \tag{13}$$

The boundary conditions at the explicit scheme can be considered the same as in the Crank-Nicolson, both at the center and at the outer surface (Eq. 6 and 8, respectively).

In the same way as in Eq. 12, the stability condition for mass diffusion need to be considered.

Also, the internal elements for mass diffusion can be calculated by an expression similar to Eq. 13:

$$\frac{X_i^{j+1} - X_i^j}{\Delta t} = \frac{2D_{ef}}{\Delta r^2}\left(X_{i+1}^j - 2X_i^j + X_{i-1}^j\right) \tag{14}$$

The boundary conditions for mass diffusion by using the explict method are the same as in Eq. 9 and 11.

2.3 Dufort-Frankel scheme

The Dufort–Frankel scheme [21–23] is a three-time explicit and unconditionally stable method. Throughout this discretization, an implicit calculation—e.g. Crank-Nicolson scheme—was used to obtain the temperate of the nodes at $j = 2$. After this initial calculation, the internal temperatures via the Dufort–Frankel scheme can be obtained with the following expression from Eq. 1:

$$\frac{T_i^{j+1} - T_i^j}{\Delta t} = \frac{\alpha}{r\Delta r^2}\left[r_{i-\frac{1}{2}}T_{i-1}^j - r_i\left(T_i^{j-1} + T_i^{j+1}\right) + r_{i+\frac{1}{2}}T_{i+1}^j\right] \tag{15}$$

The boundary conditions for heat diffusion via Dufort-Frankel method for $r = 0$ and $r = R$ are the same as in Eq. 6 and 8, respectively.

For mass transfer, the discretization of Eq. 2 via the Dufort-Frankel scheme in space and forward difference in time can be expressed as

$$\frac{X_i^{j+1} - X_i^j}{\Delta t} = \frac{D_{ef}}{r\Delta r^2}\left[r_{i+\frac{1}{2}}X_{i+1}^j - \left(r_{i-\frac{1}{2}} + r_{i+\frac{1}{2}}\right)X_i^j + r_{i-\frac{1}{2}}X_{i-1}^j\right] \tag{16}$$

The boundary condition at the center of the banana ($r = 0$) can be obtained with the approximation $X_i^j = (X_i^{j-1} + X_i^{j+1})/2$ and central difference in time:

$$\frac{X_i^{j+1} - X_i^{j-1}}{2\Delta t} = \frac{2D_{ef}}{\Delta r^2}\left[X_{i-1}^{j} - (X_i^{j-1} + X_i^{j+1}) + X_{i+1}^{j}\right] \tag{17}$$

Finally, the boundary condition at the outer surface is the same as in Eq. 11.

3 Results and Discussion

The results obtained for each scheme are illustrated in Fig. 2. The schemes were compared using the Mean Average Error (MAE), the Mean Average Percentual Error (MAPE), the Root Mean Square Error (RMSE) and the Pearson correlation coefficient (R), based on the experimental data available on the work of Pérez [24], as shown in Table 1. These coefficients were obtained by Eq. 18– 21, where τ_0^j is the experimental temperature in the center of the banana ($r = 0$) on time step j, T_0^j is the numerical temperature in the center of the banana on time step j, n_t is the total number of time steps, and $\overline{T}_0$ is the average temperature in the center of the banana.

$$\text{MAE} = \frac{1}{n_t}\sum_{j=1}^{n_t}\left|\tau_0^j - T_0^j\right| \tag{18}$$

$$\text{MAPE} = \frac{1}{n_t}\sum_{j=1}^{n_t}\left|\frac{\tau_0^j - T_0^j}{\tau_0^j}\right| \times 100 \tag{19}$$

$$\text{RMSE} = \sqrt{\frac{1}{n_t}\sum_{j=1}^{n_t}\left(\tau_0^j - T_0^j\right)^2} \tag{20}$$

$$\text{R} = \sqrt{\frac{\sum_{j=1}^{n_t}\left(T_0^j - \overline{T}_0\right)^2}{\sum_{j=1}^{n_t}\left(\tau_0^j - \overline{T}_0\right)^2}} \tag{21}$$

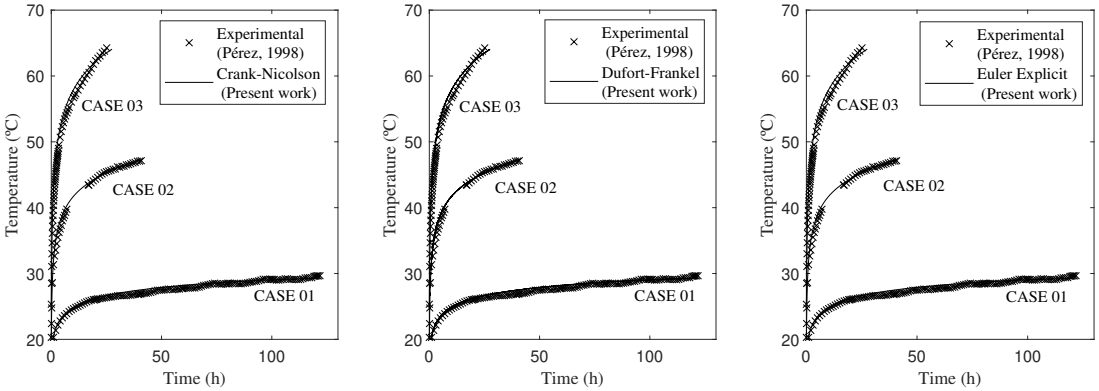

Figure 2. Comparison of the results obtained for the temperature in the center of the banana with experimental data for validation.

All three methods presented good fits for the model, with similar error coefficients. The same correlation coefficient (R) was reached for the first and second case, yet the Dufort-Frankel (DF) and the Euler Explicit (EE) schemes showed lower mean average errors for Case 01 and Case 02, respectively. It is relevant to mention that, although DF is unconditionally stable, it displayed numerical noise with an order of magnitude of 10^{-3} °C. Nevertheless, as shown in Tab 1, there was no discrepancies between schemes, and there is no relevant difference in terms of average errors.

Table 1. Comparison of MAE, MAPE, RMSQ e R for each scheme.

Case	Error	Crank-Nicholson	Dufort-Frankel	Euler explicit
Case 01	MAE	0.2783	0.2775	0.2780
	MAPE (%)	1.0230	1.0202	1.0219
	RMSE	0.3280	0.3272	0.3277
	R	0.9931	0.9931	0.9931
Case 02	MAE	0.3805	0.3847	0.3794
	MAPE (%)	1.0234	1.0445	1.0217
	RMSE	0.5886	0.5949	0.5865
	R	0.9979	0.9979	0.9979
Case 03	MAE	1.5492	1.5834	1.5427
	MAPE (%)	3.3810	3.4697	3.3655
	RMSE	1.7275	1.7735	1.7198
	R	0.9960	0.9958	0.9959

For case 03, there was a slight increase on the mean average error. Even if EE presented a lower MAE, MAPE and RMSE, the best correlation coefficient was given by the Crank-Nicolson (CN) scheme. Nonetheless, the error coefficients showed no significant difference.

The values for thermal diffusivity obtained were in the range between 2.3406×10^{-8} and $9.9225\times10^{-11}m^2/s$, which agrees with the work of Mariani *et al.* [5].

4 Conclusions

As shown by the similar error metrics, all three schemes have presented satisfactory results. Although it was not studied the effect of different mesh or time efficiency, these data prove that the schemes studied are suitable for this kind of simulation. The comparisons around time and computer efficiency for this simulation are yet to be made.

Acknowledgements. The authors would like to acknowledge and thank CAPES(Coordenação de Aperfeiçoamento de Pessoal de Nível Superior) and CNPq (Conselho Nacional de Desenvolvimento Científico e Técnológico) for the financial support.

Authorship statement. The authors hereby confirm that they are the sole liable persons responsible for the authorship of this work, and that all material that has been herein included as part of the present paper is either the property (and authorship) of the authors, or has the permission of the owners to be included here.

References

[1] A. Sharma, C. Chen, and N. V. Lan. Solar-energy drying systems: A review. *Renewable and Sustainable Energy Reviews*, vol. 13, n. 6-7, pp. 1185–1210, 2009.

[2] A. Menon, V. Stojceska, and S. A. Tassou. A systematic review on the recent advances of the energy efficiency improvements in non-conventional food drying technologies. *Trends in Food Science & Technology*, vol. 100, pp. 67–76, 2020.

[3] C. L. Hii, S. V. Jangam, S. P. Ong, and A. S. Mujumdar. Solar drying: Fundamentals, applications and innovations. *TPR Group Publication, Singapore*, vol. , 2012.

[4] M. A. Karim and M. N. A. Hawlader. Drying characteristics of banana: Theoretical modelling and experimental validation. *Journal of Food Engineering*, vol. 70, n. 1, pp. 35–45, 2005.

[5] V. C. Mariani, A. G. B. De Lima, and dos L. Santos Coelho. Apparent thermal diffusivity estimation of the banana during drying using inverse method. *Journal of Food Engineering*, vol. , pp. 569–579, 2008.

[6] W. Wang, G. Chen, and A. S. Mujumdar. Physical interpretation of solids drying: An overview on mathematical modeling research. *Drying Technology*, vol. 25, n. 4, pp. 659–668, 2007.

[7] A. M. Castro, E. Y. Mayorga, and F. L. Moreno. Mathematical modelling of convective drying of fruits: A review. *Journal of Food Engineering*, vol. 223, pp. 152–167, 2018.
[8] K. J. Park, Z. Vohnikova, and F. P. R. Brod. Evaluation of drying parameters and desorption isotherms of garden mint leaves (*Mentha crispa L.*). *Journal of Food Engineering*, vol. 51, n. 3, pp. 193–199, 2002.
[9] W. P. da Silva, C. M. Silva, D. D. Silva, and C. D. Silva. Numerical simulation of the water diffusion in cylindrical solids. *International Journal of Food Engineering*, vol. 4, n. 2, 2008a.
[10] W. P. da Silva, M. E. Mata, C. D. Silva, M. A. Guedes, and A. G. Lima. Determinação da difusividade e da energia de ativação para feijão macassar (*Vigna unguiculata (L.) Walp.*), variedade sempre-verde, com base no comportamento da secagem. *Engenharia Agrícola*, vol. 28, pp. 325–333, 2008b.
[11] W. P. da Silva, J. W. Precker, and others. Determination of the effective diffusivity via minimization of the objective function by scanning: Application to drying of cowpea. *Journal of Food Engineering*, vol. 95, n. 2, pp. 298–304, 2009.
[12] W. P. da Silva, e C. M. Silva, V. S. Farias, and J. P. Gomes. Diffusion models to describe the drying process of peeled bananas: Optimization and simulation. *Drying Technology*, vol. 60, n. 2, pp. 164–174, 2012.
[13] W. P. da Silva, I. Hamawand, and e C. M. Silva. A liquid diffusion model to describe drying of whole bananas using boundary-fitted coordinates. *Journal of Food Engineering*, vol. 137, pp. 32–38, 2014.
[14] A. G. B. de Lima, M. R. Queiroz, and S. A. Nebra. Simultaneous moisture transport and shrinkage during drying of solids with ellipsoidal configuration. *Chemical Engineering Journal*, vol. 86, n. 1-2, pp. 85–93, 2002.
[15] W. P. da Silva, e C. M. Silva, e D. D. Silva, de G. Araújo Neves, and de A. G. B. Lima. Mass and heat transfer study in solids of revolution via numerical simulations using finite volume method and generalized coordinates for the cauchy boundary condition. *International Journal of Heat and Mass Transfer*, vol. 53, n. 5-6, pp. 1183–1194, 2010.
[16] H. Janssen. Simulation efficiency and accuracy of different moisture transfer potentials. *Journal of Building Performance Simulation*, vol. 7, n. 5, pp. 379–389, 2014.
[17] F. Tariku, K. Kumaran, and P. Fazio. Transient model for coupled heat, air and moisture transfer through multilayered porous media. *International Journal of Heat and Mass Transfer*, vol. 53, n. 15-16, pp. 3035–3044, 2010.
[18] J. Crank and P. Nicolson. A practical method for numerical evaluation of solutions of partial differential equations of the heat-conduction type. In *Mathematical Proceedings of the Cambridge Philosophical Society*, volume 43, pp. 50–67. Cambridge University Press, 1947.
[19] M. N. Özişik, H. R. Orlande, M. J. Colaco, and R. M. Cotta. *Finite difference methods in heat transfer*. CRC Press, 2017.
[20] H. P. Langtangen and S. Linge. *Finite difference computing with PDEs: A modern software approach*. Springer Nature, 2017.
[21] L. Wu. DuFort–Frankel-type methods for linear and nonlinear Schrödinger equations. vol. 33, n. 4, pp. 1526–1533, 1996.
[22] S. Gasparin, J. Berger, D. Dutykh, and N. Mendes. Stable explicit schemes for simulation of nonlinear moisture transfer in porous materials. *Journal of Building Performance Simulation*, vol. 11, n. 2, pp. 129–144, 2018.
[23] D. A. Anderson, J. C. Tannehill, R. H. Pletcher, M. Ramakanth, and V. Shankar. *Computational fluid mechanics and heat transfer*. CRC Press, 2020.
[24] V. Haber Perez. Estudo do comportamento da temperatura de bananas durante o processo de secagem. Master's thesis, Universidade Estadual de Campinas. Faculdade de Engenharia Agricola, 1998.